Image deblurring using empirical Wiener filter in the curvelet domain and joint non-local means filter in the spatial domain

H Yang*[a,b], Z B Zhang[b], D Y Wu[b] and H Y Huang[b]
[a]Institute of Optics, Fine Mechanics and Physics Institute, Chinese Academy of Sciences, Changchun 130033, China

[b]School of Mathematics, Jilin University, Changchun 130012, China

Abstract: In this paper, an efficient image deblurring algorithm is proposed. This algorithm restores the blurred image by incorporating a curvelet-based empirical Wiener filter with a spatial-based joint non-local means filter. Curvelets provide a multidirectional and multiscale decomposition that has been mathematically shown to represent distributed discontinuities such as edges better than traditional wavelets. Our method restores the image in the frequency domain to obtain a noisy result with minimal loss of image components, followed by an empirical Wiener filter in the curvelet domain to attenuate the leaked noise. Although the curvelet-based methods are efficient in edge-preserving image denoising, they are prone to producing edge ringing which relates to the structure of the underlying curvelet. In order to reduce the ringing, we develop an efficient joint non-local means filter by using the curvelet deblurring result. This filter could suppress the leaked noise while preserving image details. We compare our deblurring algorithm with a few competitive deblurring techniques in terms of improvement in signal-to-noise-ratio (ISNR) and visual quality.

Keywords: image deblurring, curvelets, non-local means filter, empirical Wiener filter

1 INTRODUCTION

Image deblurring is a classical inverse problem; the goal of it is to best estimate an image that has been degraded. Such inverse problems often arise in many image processing applications such as radiometry, satellite imaging, optical systems, magnetic resonance imaging and seismic processing. Deblurring becomes necessary when we wish a crisp deblurred image for viewing or further processing.

Wavelets are popular for image representation and are used in a wide variety of image processing applications such as compression, and image restoration.[1] The main reason for wavelets' success can be explained by their ability to sparsely represent one-dimensional signals which are smooth away from point discontinuities. It is because of this optimality property of wavelet representations that wavelet-based deblurring routines have been proposed. However, wavelet representations are actually not optimal for all types of images. Specifically, in dimension two, if we model images as piecewise smooth functions that are smooth away from a C^2 edge, the standard two-dimensional (2D) wavelets do not reach the best possible rate. As a result, denoising estimates based on 2D wavelets tend to have small unwanted artefacts and complex decision metrics or schemes need to be utilised to try to improve the quality of the estimate. In particular, the approximation

The MS was accepted for publication on 30 July 2010.
* *Corresponding author: Hang Yang, Institute of Optics, Fine Mechanics and Physics Institute, Chinese Academy of Sciences, Dongnanhu 3888, Changchun 130033, China; email: yanghang09@mails.jlu.edu.cn*

error for a wavelet representation decays as $O(N^{-1})$ as N increases.[2] Multidirectional representations such as curvelets[3–5] can provide nearly the optimal approximation rate for these types of images [the approximation rate being $O(N^{-2}(\log N)^3)$ as N increases[6]]. The curvelet transform is tailored to exploit the structure of images, such as seismic images,[5,7] which contain directionally oriented features. In this work, we utilise unique properties to an implementation of the curvelet transform that offer advantages for the purpose of deblurring.

The concept of using a sparse representation to achieve good estimates for deblurring has been suggested before (see, for example, Ref. 8). However, particular features concerning implementations of such representations that contribute to performance presented here have not been previously considered. The performance of the proposed method is improved by using an empirical Wiener shrinkage filter. In this case, the curvelet coefficients with a slightly different decomposition are filtered using the initial curvelet-based estimate.

In the implementation stage, to surmount the problems of boundary effects, and to be effective in regularising the approximate deblurring process, a joint non-local means (NLM) filter is utilised. The NLM filter[9,10] replaces a pixel's value by a weighted average of pixels selected using self-similarity for image denosing. This method has shown remarkable and convincing results. Our joint NLM filter modifies the NLM filter using a reference image to achieve a texture-preserving result.

1.1 Problem statement

The degradation procedure is often modelled as the result of a convolution with a low-pass filter

$$\begin{aligned} y(n_1,n_2) &= \mathcal{H}x(n_1,n_2)+\gamma(n_1,n_2) \\ &= (h \circledast x)(n_1,n_2)+\gamma(n_1,n_2) \end{aligned} \tag{1}$$

where x and y are the original image and the observed image, respectively. γ is the noise introduced in the procedure of image acquisition, and it is generally assumed to be independent and identically distributed zero-mean additive white Gaussian noise (AWGN) with variance σ^2. $\circledast$ denotes circular convolution, and h denotes the point spread function (PSF) of a linear space invariant system $\mathcal{H}$.

A naive deblurring estimate $\bar{x}$ is obtained using the operator inverse $\mathcal{H}^{-1}$ as:

$$\bar{x}(n_1,n_2) = \mathcal{H}^{-1}y(n_1,n_2) = x(n_1,n_2)+\mathcal{H}^{-1}\gamma(n_1,n_2)$$

Unfortunately, the variance of the colored noise $\mathcal{H}^{-1}\gamma$ in $\bar{x}$ is large when $\mathcal{H}$ is ill conditioned. Thus, to get a reasonable image estimate, a method of reducing/controlling noise needs to be utilised.

1.2 Known approaches

In recent years, lots of deblurring algorithms have been proposed. In these methods, the Wiener filter[11,12] and the constrained least squares algorithm,[11] can solve this problem in the frequency domain in a fast speed. However, they often obtain a noisy result with ringing effects. Increased performance of deblurring methods can be attributed to the inclusion of the wavelet-based estimators. One such technique called the wavelet-vaguelette deconvolution was proposed in Ref. 13, and an improved hybrid wavelet-based regularised deblurring algorithm that works with any ill-conditioned convolution system was developed in Ref. 14. This Fourier-wavelet regularised deconvolution (ForWaRD) method can obtain good results via tandem scalar shrinkages in both the Fourier and wavelet domains. However, sometimes the restored images would have slightly low contrast and ripple artefacts. An extension in shearlet and incomplete measurements, named as ShearDec and ForIcM, was proposed in Refs. 15 and 16, respectively.

The iterative deblurring method is another important category.[17–19] The well-known basic iterative methods are Landweber[20] and Richardson–Lucy.[21,22] Many extensions and improvements over these methods have been proposed that include use of the wavelets or other sparse representations, such as contourlets.[23,24] The fast total variation deconvolution (FTVd) method,[25] which is well known for its edge-preserving capability, can generally achieve state-of-the-art results, and some iterative methods for total variation-based image restoration can be found in Refs. 26–28. The total variation deblurring method finds approximate solutions to differential equations in the space of bounded variation functions. The space of bounded variation functions is a reasonable functional model for images since it contains piecewise smooth functions that allow for discontinuities. The discontinuities can be identified as the image edges. However, its ability to describe image textures is not satisfactory. This method usually leads to a slightly blocky result and some fine image textures are lost. Because image textures are important visual information to the human eye, the results with texture loss may show unnatural looks.

The Imaging Science Journal ims356.3d 20/8/12 17:04:41
The Charlesworth Group, Wakefield +44(0)1924 369598 - Rev 7.51n/W (Jan 20 2003)

1.3 Proposed algorithm

In this paper, we develop an efficient algorithm that combines the curvelet-based empirical Wiener filter and the spatial-based joint NLM filter for image deblurring. We adopt a three-step non-iterative processing procedure, which first uses regularisation in the Fourier domain to restore a noisy result, and then following an empirical Wiener shrinkage filter in curvelet domain, finally, considering that the curvelet deblurring image preserves most of the important image features, we use it as a reference image in the spatial denoising for the noisy image obtained from the first step. Therefore, an efficient joint NLM filter is developed. Compared with other spatial algorithms, this proposed spatial filter could suppress the noise while preserving image details.

1.4 Paper organisation

In Section 2, we give a brief introduction to the curvelet transform. In Section 3, we discuss details about the proposed deblurring algorithm. In Section 4, we show some of the simulation results, and present the concluding remarks in Section 5.

2 AN OVERVIEW OF CURVELET TRANSFORM

Curvelets are new multiscale transforms that represent an image in terms of shifted versions of a low-pass scaling function and shifted, dilated and rotated versions of a prototype band-pass curvelet function. Unlike wavelet basis functions, each band-pass curvelet basis function has an elongated envelope with the envelope's length scaling as its width squared; this is referred to as the parabolic scaling law.[4] The curvelet transform was designed to represent edges and other singularities along curves much more efficiently than traditional transforms. Formally, curvelets provide optimally economical representations for images in so-called C^2/C^2 spaces. An C^2/C^2 image comprises twice differentiable regions separated by piecewise twice differentiable boundary curves. In other words, an C^2/C^2 image is a piecewise 'smooth' image with piecewise 'smooth' boundary edges.[4]

In this paper, we use a so-called second-generation discrete curvelet transform,[5] which is extremely simple to use.

Let μ be the collection of triple index (j,l,k), where j, l and $k=(k_1,k_2)\in Z^2$ are respectively scale, orientation and translation parameters. The curvelets are defined as functions of $x\in R^2$ by

$$\varphi_\mu(x)=\varphi_{\mathrm{j,l,k}}(x)=\varphi_{\mathrm{j}}\left[R_{\theta_{\mathrm{l}}}\left(x-x_{\mathrm{k}}^{(\mathrm{j,l})}\right)\right]$$

where $\theta_{\mathrm{l}}=2\pi 2^{-\lfloor \mathrm{j}/2\rfloor}l$, with $l=0, 1, \ldots$ such that $0\leqslant\theta_{\mathrm{l}}<2\pi$, $x_{\mathrm{k}}^{(\mathrm{j,l})}=R_{\theta_{\mathrm{l}}}^{-1}\left(k_1 2^{-\mathrm{j}},k_2 2^{-\mathrm{j}/2}\right)$, R_θ is the rotation by θ radians and R_θ^{-1} is its inverse. In the above, φ is a waveform which is oscillatory in the horizontal direction and bell-shaped along the vertical direction.

A curvelet coefficient is then simply the inner product between an element $f\in L^2\left(R^2\right)$ and a curvelet φ_μ,

$$c_\mu=C_\mu f=\langle f,\varphi_\mu\rangle=\int_{\mathrm{R}^2} f(x)\overline{\varphi}_\mu(x)\mathrm{d}x \tag{2}$$

which can be evaluated directly in frequency domain. Here $\overline{\varphi}_\mu$ is the conjugation of φ_μ. Introduce the 2D frequency window

$$U_{\mathrm{j}}(\omega)=2^{-3\mathrm{j}/4}W\left(2^{-\mathrm{j}}|\omega|\right)V\left(\frac{2^{\lfloor \mathrm{j}/2\rfloor}\theta}{2\pi}\right)$$

where the radial window W (e.g. Meyer wavelet window) partitions the frequency domain into annuli $|x|\in[2^{\mathrm{j}}, 2^{\mathrm{j}+1})$ and the angular window V partitions the annuli into wedges θ_l. By defining the curvelets in the frequency domain $\widehat{\varphi}_\mu(\omega)=U_{\mathrm{j}}(R_{\theta_{\mathrm{l}}})e^{-\langle x_{\mathrm{k}}^{\mathrm{j,l}},\omega\rangle}$. Taking oriented local Fourier bases on each wedge, and using Plancherel's theorem for equation (2), we get

$$c_\mu=\frac{1}{(2\pi)^2}\int\hat{f}(\omega)U_{\mathrm{j}}(R_{\theta_{\mathrm{l}}})e^{\langle x_{\mathrm{k}}^{(\mathrm{j,l})},\omega\rangle}\mathrm{d}\omega$$

There are two digital implementations of the curvelet transform in two dimensions.[5] The first digital transformation is based on unequally spaced fast Fourier transforms, while the second is based on the wrapping of specially selected Fourier samples (Wrapping). Both implementations are fast in the sense that they run in $O(M^2\log M)$ for an $M\times M$ image. In addition, they are also invertible, with rapid inversion algorithms of about the same complexity. For details, we refer to Ref. 5. In this paper, the digital transformation based on 'Wrapping' is used in the experiments.

3 EMPIRICAL WIENER FILTER AND JOINT NLM FILTER

3.1 Fourier-based deblurring

The Fourier domain is the traditional choice for deblurring[11] because convolution simplifies to scalar Fourier operations and it provides the most economical

The Imaging Science Journal ims356.3d 20/8/12 17:04:42
The Charlesworth Group, Wakefield +44(0)1924 369598 - Rev 7.51n/W (Jan 20 2003)

representation of the colored noise $\mathcal{H}^{-1}\gamma$.[14] That is, equation (1) can be rewritten as

$$Y(k_1,k_2)=H(k_1,k_2)X(k_1,k_2)+\Gamma(k_1,k_2) \tag{3}$$

where Y, X, H and Γ are the 2D discrete Fourier transforms (DFTs) of y, x, h and γ, respectively. Rewriting the pseudo-inversion operation in the Fourier domain

$$\tilde{X}(k_1,k_2)=\begin{cases} X(k_1,k_2)+\Gamma(k_1,k_2)/H(k_1,k_2), & \text{if } |H(k_1,k_2)|>0, \\ 0, \text{ otherwise} \end{cases} \tag{4}$$

where $\tilde{X}$ is the DFT of $\tilde{x}$. Equation (4) clearly demonstrates that noise components where $|H(k)|\approx 0$ are particularly amplified during operator inversion.

In our method, we first employ the simplified linear time invariant (LTI) Wiener shrinkage[29] to obtain a distortion-free but noisy estimate. As reported in Ref. 14, this LTI Wiener shrinkage is sufficient to significantly attenuate the amplified noise components with a minimal loss of image components. When an estimate of the power spectral density can be accurately determined from a method such as that proposed in Ref. 29, a LTI Wiener-based solution can be found by using

$$\mathbf{H}_\alpha(k_1,k_2)=\frac{\overline{H}(k_1,k_2)}{|H(k_1,k_2)|^2+\alpha[M^2\sigma^2/|Psd(k_1,k_2)|]} \tag{5}$$

where σ^2 is the variance of noise, $\alpha\in R^+$, Psd is the estimated power spectral density of the image, $\overline{H}$ is the complex conjugate of H and M is the size of image. An image estimate in the Fourier domain can be written by

$$\begin{aligned} X_\alpha(k_1,k_2) &= Y(k_1,k_2)\mathbf{H}_\alpha(k_1,k_2) \\ &= X(k_1,k_2)\frac{\overline{H}(k_1,k_2)}{|H(k_1,k_2)|^2+\alpha[M^2\sigma^2/|Psd(k_1,k_2)|]}+\Gamma_\alpha \end{aligned} \tag{6}$$

$$\Gamma_\alpha=\Gamma(k_1,k_2)\mathbf{H}_\alpha(k_1,k_2)$$

The X_α and $\Gamma\mathbf{H}_\alpha$ denote the respective DFTs of the estimate image x_α and the leaked noise γ_α.

Consequently, after the LTI Wiener shrinkage step (equation (6)), the leaked noise γ_α in the x_α has substantially reduced variances $\sigma^2_{\alpha,\mu}$ in all curvelet coefficients. The variance $\sigma^2_{\alpha,\mu}$ at curvelet subscript μ is given by

$$\sigma^2_{\alpha,\mu}=\mathbf{E}\left(|\langle\gamma_\alpha,\varphi_\mu\rangle|^2\right)=$$

$$\sigma^2\sum_{k_1,k_2}\left|\frac{\overline{H}(k_1,k_2)}{|H(k_1,k_2)|^2+\alpha[M^2\sigma^2/|Psd(k_1,k_2)|]}\Psi_\mu(k_1,k_2)\right|^2 \tag{7}$$

where Ψ_μ is the DFT of curvelet φ_μ.

3.2 Curvelet-based empirical Wiener filter

The remaining aspect of the deblurring problem is transformed into a denoising problem in the presence of leaked noise. Curvelets offer a better representation of images containing directionally oriented features than traditional transforms, and the empirical Wiener shrinkage in the curvelet domain can provide well estimates of x.

In the case when wavelets are used for image denoising, it was shown in Ref. 30 that an empirical Wiener wavelet shrinkage filter typically improves upon the mean square error performance over that of hard/soft thresholding. By the empirical Wiener shrinkage, we mean to weigh the curvelet coefficients as

$$c^{\mathrm{w}}_{\alpha,\mu}=c_{\alpha,\mu}\frac{|c^{\mathrm{e}}_{\alpha,\mu}|^2}{|c^{\mathrm{e}}_{\alpha,\mu}|^2+\lambda\sigma^2_{\alpha,\mu}} \tag{8}$$

where $c^{\mathrm{e}}_{\alpha,\mu}$ are the curvelet coefficients from another denoised estimate, $\sigma^2_{\alpha,\mu}$ are the noise's variance at curvelet subscript μ and λ is regularisation parameters. The performance of the proposed method is improved by using this empirical Wiener shrinkage filter. In this case, we use two different decompositions (different decomposition scales and different decomposition orientations). We denote the curvelet coefficients using the different subscripts μ' and μ for the different decompositions, respectively (for one curvelet transform implementation, we used 1, 8, 16, 16, 32 and 32 directions in the scales from coarse to fine; for the other curvelet transform implementation, we used 1, 16, 32, 32, 64 and 64 directions in the scales from coarse to fine).

To attenuate the leaked noise, the hard-threshold is first made dependent on the variance of each curvelet-transform coefficient using the curvelet decomposition μ'. Let $c_{\alpha,\mu'}$ denote the curvelet coefficients of the still noisy image x_α for a given regularisation parameter α and subscript μ'. We shrink $c_{\alpha,\mu'}$ with the hard-thresholding function $HT\left(c_{\alpha,\mu'},\rho\right)$ to obtain $c^{\mathrm{e}}_{\alpha,\mu'}$.

$$HT\left(c_{\alpha,\mu'},\rho\right)=\begin{cases} c_{\alpha,\mu'}, & \text{if } |c_{\alpha,\mu'}|>\rho\sigma^2_{\alpha,\mu'}, \\ 0, & \text{otherwise} \end{cases} \tag{9}$$

Then we compute the inverse curvelet transform with the $c^{\mathrm{e}}_{\alpha,\mu'}$ to obtain an initial curvelet-based estimate x^{e}_α.

Then, we use the x^{e}_α to construct the c^{w}_μ. Let $c_{\alpha,\mu}$ and $c^{\mathrm{e}}_{\alpha,\mu}$ denote the curvelet coefficients of the still noisy image x_α and the 'empirical' estimate x^{e}_α using curvelet decomposition μ, respectively. Using equation (8), we can obtain the empirical Wiener curvelet

The Imaging Science Journal ims356.3d 20/8/12 17:04:43
The Charlesworth Group, Wakefield +44(0)1924 369598 - Rev 7.51n/W (Jan 20 2003)

coefficients. Computing the inverse curvelet transform with $c^{w}_{\alpha,\mu}$, we can get the curvelet-based empirical Wiener estimate x^{w}_{α}.

The estimate $c^{e}_{\alpha,\mu} = C_{\mu}x^{e}_{\alpha} = C_{\mu}C^{T}_{\mu'}c^{e}_{\alpha,\mu'}$. The mismatch between C_{μ} and $C_{\mu'}$ guarantees that the operator $C_{\mu}C^{T}_{\mu'}$ spreads or stretches the clear image trustworthy coefficients in $c^{e}_{\alpha,\mu'}$ into a larger number of nonzero coefficients in $c^{e}_{\alpha,\mu}$. The composite operator $C_{\mu}C^{T}_{\mu'}$ smooths $c^{e}_{\alpha,\mu'}$ to predict the remaining noise dubious coefficients, and yields an estimate of the noisy image coefficients. The empirical Wiener filter designed using the same curvelet decomposition almost completely coincides with the hard thresholding filter.[30]

An important advantage in the use of the curvelet transform implementation for deblurring is that it has the ability to represent edges and other singularities along curves much more efficiently than traditional transforms. The needle-shape elements of curvelets also own very high directional sensitivity and anisotropy. Obviously, it is natural to apply the curvelet for detail-preserving image deblurring.

3.3 Joint NLM filter in spatial domain

As mentioned above, curvelet-based methods produce edge ringing which relates to the structure of the underlying curvelet, and most spatial-based algorithms output much higher quality denoising image with less artifacts. The NLM filter, as described in Refs. 9, 10 and 31, applied a simple nonlinear filter to remove noise while retaining the sharpness of edges. Nonlocal methods are an exciting innovation and work well for texture-like images containing many repeated patterns. Given a noisy image u, at a pixel location (i,j), the restored result $\hat{u}(i,j)$ can be directly calculated by a weighted average of the intensities in its noisy neighbourhood $u(k,l)$ as follows:

$$\hat{u}(i,j) = \sum_{(k,l)\in\Omega_{P}(i,j)} \omega([k,l],[i,j])u(k,l) \tag{10}$$

where the weights $\{\omega([k,l],[i,j])\}_{k,l}$ are defined as,

$$\omega([k,l],[i,j]) = \frac{1}{C_{i,j}}\exp\left(-\frac{\left\|u(N_{i,j}) - u(N_{k,l})\right\|^{2}_{2,a}}{\sigma^{2}_{h}}\right) \tag{11}$$

$$\left\|u(N_{i,j}) - u(N_{k,l})\right\|^{2}_{2,a} = \sum_{m=-L}^{L}\sum_{n=-L}^{L} G_{a}(m,n)\left[u(N_{i,j})(m,n) - u(N_{k,l})(m,n)\right]^{2} \tag{12}$$

and the $\Omega_{P}(i,j)$ denotes the set of points in the $(2P+1)\times(2P+1)$ window centered at (i,j), $(2L+1)\times(2L+1)$ is the size of similarity square neighbourhood window, $u(N_{i,j})$ is the image patch centered at pixel location (i, j) and G_{a} is a Gaussian kernel, where a is the standard deviation. σ_{h} is the similarity spread in the image range. $C_{i,j}$ is the normalisation factor. $\|u(N_{i,j}) - u(N_{k,l})\|^{2}_{2,a}$ is the weighted Euclidean distance of the two pixels' neighbourhoods $N_{i,j}$ and $N_{k,l}$ with equal size.

This formula amounts to say that the denoised value at (i,j) is a mean of the values of all points whose gaussian neighbourhood looks like the neighbourhood of (i,j). Rather than simply replacing a pixel's value with a weighted average of its neighbours in the image domain, this filter replaces a pixel's value by a weighted average of pixels selected using self-similarity to achieve a texture-preserving result.

The parameter a characterises the spatial behavior of the filter, but with the changes of the noise level and the size of Ω_{P}, a is not easy to select. So we define a simpler spatial weight function D to replace the Gaussian kernel G_{a}

$$D(m,n) = \sum_{d=s}^{L}\frac{1}{(2d+1)^{2}},\ s = \max(|m|,|n|,1)$$

Let $\|\bullet\|_{D}$ denote the l_{2} norm by using weight function D. That is to say, we use the weight function D to replace the function G_{a} in equation (12).

The main problem of the classic non-local filter in image denoising is that the weights could not be estimated accurately based on the noisy image. If a reference contains a much better estimate of the true high-frequency information than the noisy image,[32] we can present a joint NLM filter to compute the weights. In this way, the weights could be estimated more accurately.

Now, we propose the joint NLM algorithm, which is defined by the simple formula

$$\hat{u}(i,j) = \frac{1}{C^{ref}_{i,j}}\sum_{(k,l)\in\Omega_{P}(i,j)}\exp\left(-\frac{\|u^{ref}(N_{i,j}) - u^{ref}(N_{k,l})\|^{2}_{D}}{\sigma^{2}_{h}}\right)u(i,j) \tag{13}$$

Considering that the curvelet deblurring image preserves most of the important image textural features, we use it as a reference image in the spatial denoising. So the proposed joint NLM filter is very efficient to improve the image quality. Then, the restored result x^{J} using joint NLM filter can be calculated as follow:

The Imaging Science Journal ims356.3d 20/8/12 17:04:44
The Charlesworth Group, Wakefield +44(0)1924 369598 - Rev 7.51n/W (Jan 20 2003)

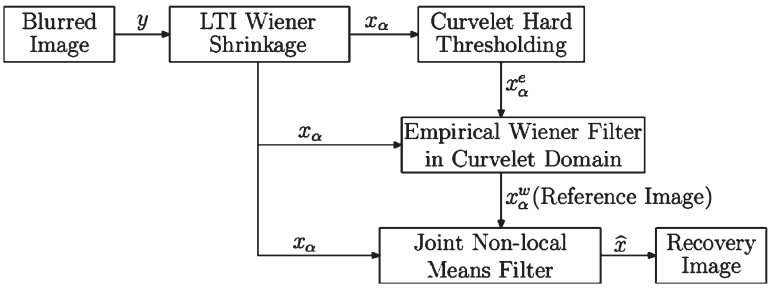

1 Block-diagram of our algorithm

$$x^{\mathrm{J}}(i,j) = \frac{1}{C^{\mathrm{ref}}_{\mathrm{i,j}}} \sum_{(\mathrm{k,l})\in\Omega_{\mathrm{P}}(\mathrm{i,j})} \exp\left(-\frac{\|x^{\mathrm{w}}_{\alpha}(N_{\mathrm{i,j}}) - x^{\mathrm{w}}_{\alpha}(N_{\mathrm{k,l}})\|^2_{\mathrm{D}}}{\sigma^2_{\mathrm{h}}}\right) x_\alpha(i,j) \tag{14}$$

where x^{w}_{α} is the curvelet-based estimate.

If we use the joint NLM filter in equation (14) directly, there are some noise spots in the output debluring image, especially when the noise level is high. In this paper, for simplicity, we add the curvelet-based estimate in the joint NLM filter to suppress the spots.

$$\hat{x} = \beta x^{\mathrm{w}}_{\alpha} + (1-\beta)x^{\mathrm{J}},\ \beta\in[0,\ 1) \tag{15}$$

This method also can balance the curvelet-based estimate and joint NLM-based estimate, and improve the image quality.

3.4 Deblurring algorithm

We summarise the main steps of the proposed image deblurring algorithm as follows (Fig. 1):

3.4.1 Step 1. Operator inversion and Fourier shrinkage

Obtain Y and H by computing the DFTs of y and h. Then, apply the LTI Wiener filter $\mathbf{H}_\alpha$ (equation (5)) to Y to obtain X_α. Compute the inverse DFT of X_α to obtain x_α.

3.4.2 Step 2. Curvelet-based empirical Wiener filter

1. Compute the curvelet transform of still noisy image x_α to obtain $c_{\alpha,\mu'}$, and estimate the variance using equation (7). Shrink $c_{\alpha,\mu'}$ with hard-thresholding function equation (9) to obtain $c^{\mathrm{e}}_{\alpha,\mu'}$. Compute the inverse curvelet transform with the $c^{\mathrm{e}}_{\alpha,\mu'}$ to obtain an initial curvelet-based estimate x^{e}_{α}.
2. Compute the curvelet transform of still noisy image x_α and the initial curvelet-based estimate x^{e}_{α} to obtain $c_{\alpha,\mu}$ and $c^{\mathrm{e}}_{\alpha,\mu}$ using the different curvelet decomposition from the Step 2.1 (note the difference between μ and μ'.) Estimate the variance using equation (7). Use the empirical Wiener filter (equation (8)), we can obtain the empirical Wiener curvelet coefficients $c^{\mathrm{w}}_{\alpha,\mu}$. Compute the inverse curvelet transform with the $c^{\mathrm{w}}_{\alpha,\mu}$ to obtain the curvelet-based empirical Wiener estimate x^{w}_{α}.

3.4.3 Step 3. Joint NLM filter

In the spatial phase, the joint NLM filter for x_α using the previously generated curvelet restoration results x^{w}_{α} as a reference image, and then we get the final recovery image $\hat{x}$ using equations (14) and (15).

4 EXPERIMENTS

In this section, we present results of our proposed algorithm and compare them with some of the deblurring methods such as ForWaRD,[14] FTVd,[25] ShearDec,[15] L0-AbS[17] and CGMK.[18] In these experiments, we will use the improvement in signal-to-noise-ratio (ISNR) to measure the performance.

The ISNR is defined as

$$\mathrm{ISNR} = 10\log_{10}\left(\frac{\|x-y\|^2_2}{\|x-\hat{x}\|^2_2}\right)$$

In our experiments, we used the following parameter settings. In the joint NLM filter, we kept a 11×11 pixels search window and a 7×7 similarity square neighbourhood of pixels for all the results reported in this paper, that is to say, we set $P=5$ and $L=3$. For the parameter σ_{h}, we found that a large value of it would result in a smooth image, whereas a too small value would lead to inadequate denoising. The choice of this parameter is largely heuristic in nature. We have empirically found that $\sigma_{\mathrm{h}}\in[0{\cdot}025,\ 0{\cdot}05]$ generally yields good results and have accordingly used $\sigma_{\mathrm{h}}=0.04$ for the results in the experiments.

The Imaging Science Journal ims356.3d 20/8/12 17:04:44
The Charlesworth Group, Wakefield +44(0)1924 369598 - Rev 7.51n/W (Jan 20 2003)

Table 1 Description of the observation parameters for the five experiments

	Blur	σ^2
Exp 1	$h_{i,j}=(1+i^2+j^2)$, $i, j=-7, \ldots, 7$ (Barabra)	8
Exp 2	9×9 uniform kernel (Barabra)	0.308
Exp 3	$[1, 4, 6, 4, 1]^T$ [1, 4, 6, 4, 1]/256 (Barabra)	49
Exp 4	$h_{i,j}=(1+i^2+j^2)$, $i, j=-7, \ldots, 7$ (Gold Hill)	2
Exp 5	Gaussian PSF (25×25) with standard deviation 1.6 (Lena)	4
Exp 6	Gaussian PSF (35×35)with standard deviation 2.6 (Lena)	4

In our joint NLM filter, the parameters β in equation (15) vary with respect to the reference image quality. Ideally, if the reference image is very close to the original image, $\beta=0$ could be good choice. However, in fact, the reference image is generated from the noisy image by using the curvelet Wiener shrinkage filter. Experimental results show that good range for the parameter is $\beta\in[0{\cdot}3, 0{\cdot}5]$. In this paper, for simplicity, we set $\beta=0.4$. And the regularisation parameter α was estimated by the method proposed in Ref. 14. The $\lambda=3.0$ in equation (8) and $\rho=2.0$ in equation (9) for all experiments. Although better results could be obtained with 'optimal' tuning of these parameters, from our experience with this method, it is believed that these heuristic values can achieve good results in most cases.

We consider six benchmark deblurring problems. In these experiments, the original images are Barbara (experiments 1, 2 and 3) of size 512×512, Gold Hill of size 512×512 (experiment 4) and Lena of size 512×512 (experiments 5 and 6). Table 1 summarises the different degradation models used, which are defined by the blur type and the variance of the additive white Gaussian noise.

We have compared the ISNR result given by our approach and the other published state-of-the-art methods respectively in Tables 2.

In the first set of tests, the Barbara image is blurred by a PSF given by $h_{i,j}=(1+i^2+j^2)$, $i, j=-7, \ldots, 7$, and the noise variance is $\sigma^2=8$. The SNR improvements are summarised in Table 2 under the Exp 1. Our algorithm outperforms the other methods in terms of ISNR.

In the second set of tests, the Barbara image is blurred by a 9×9 uniform box-car blur. The AWGN variance is 0.308. A comparison of different methods in terms of ISNR is shown in Table 2 under the Exp 2 column. The proposed method yields a value of 5.01 dB which is better than the values obtained by any of the other methods.

In the third experiment, the original image Barbara is blurred by a 5×5 separable filter with weights [1, 4, 6, 4, 1]/16 in both the horizontal and vertical directions and then contaminated with AWGN with $\sigma^2=49$. The details of the images obtained by the different methods are shown in Fig. 2. Again, our algorithm performs the best in terms of ISNR and captures the details better than any of the other methods. Both the objective and subjective quality of our estimates are high.

In the forth set of tests, we use the blur filter considered in Exp 1. The original image of Gold Hill is blurred by this PSF, and the noise variance $\sigma^2=2$. The ISNR values are summarised in Table 2 under the Exp 4 column. The proposed method yields a value of 5.22 dB which is better than the values obtained by any of the other methods. The results obtained by different methods are shown in Fig. 3. One can see that our method achieves better visual result than the others algorithms.

In the fifth set of tests, the original image of Lena is blurred by a Gaussian PSF defined as

Table 2 ISNR for different experiments

Methods	Exp 1	Exp 2	Exp 3	Exp 4	Exp 5	Exp 6
ForWaRD	1.87	4.02	0.94	4.51	3.74	2.34
FTVd	1.67	4.63	0.67	4.98	3.63	2.61
ShearDec	2.54	4.57	1.72	4.66	3.90	2.73
L0-AbS	1.68	3.81	0.78	5.02	4.11	2.87
CGMK	1.34	3.55	0.44	4.95	3.93	2.52
Proposed method	3.97	5.01	2.27	5.22	4.27	3.08

The Imaging Science Journal ims356.3d 20/8/12 17:04:45
The Charlesworth Group, Wakefield +44(0)1924 369598 - Rev 7.51n/W (Jan 20 2003)

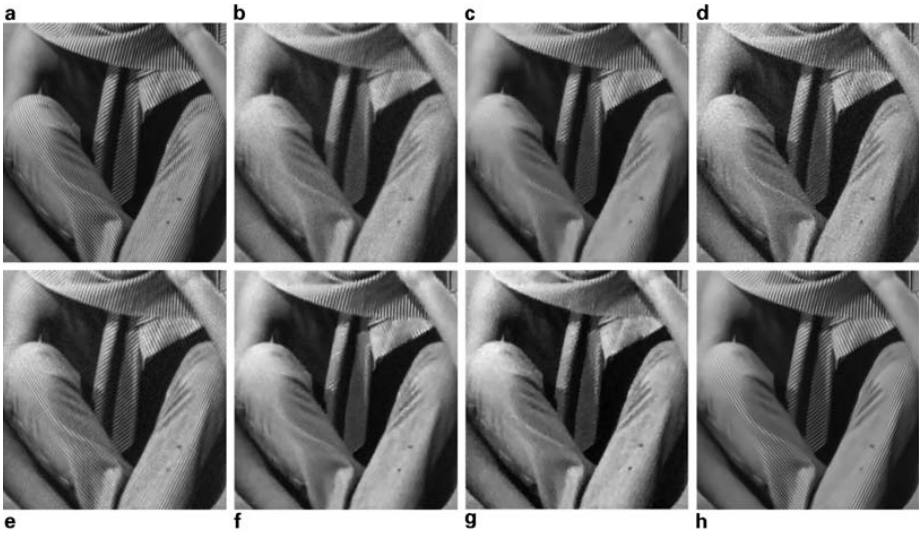

2 Details of the image deblurring experiment with a 512×512 Barbara image: (a) original image; (b) blurred image; (c) ForWaRD result; ISNR = 0.94; (d) FTVd result, ISNR = 0.67; (e) ShearDec result, ISNR = 1.72; (f) L0-AbS result, ISNR = 0.78; (g) CGMK result, ISNR = 0.44; (h) our method result, ISNR = 2.27

$$h(i,j) = K \exp\left(-\frac{i^2+j^2}{2\eta^2}\right)$$

for $i,j = -12, \ldots, 12$, where K is a normalising constant ensuring that the blur is of unit mass, and η^2 is the variance that determines the severity of the blur. In this experiment, we chose $\eta = 1.6$ and the noise variance $\sigma^2 = 4$. We report the simulation results under the Exp 5 column of Table. 2. And Fig. 4 shows the details of the images obtained by the different methods.

In the above experiments, the blur kernel and the noise variance are assumed exactly known. In practice, noise variance error on algorithm effect is very small. When an inaccurate blur kernel is used as the input, some distortions will appear in the image recovered. In light of the robustness to noise and PSF of our method shown in Fig. 5, we replicated the set-up similar to that given in Ref. 19. In many practical situations, the PSF is only partially known and the noise variance contains error. In this experiment, the Gaussian PSF used to blur the Lena image has a

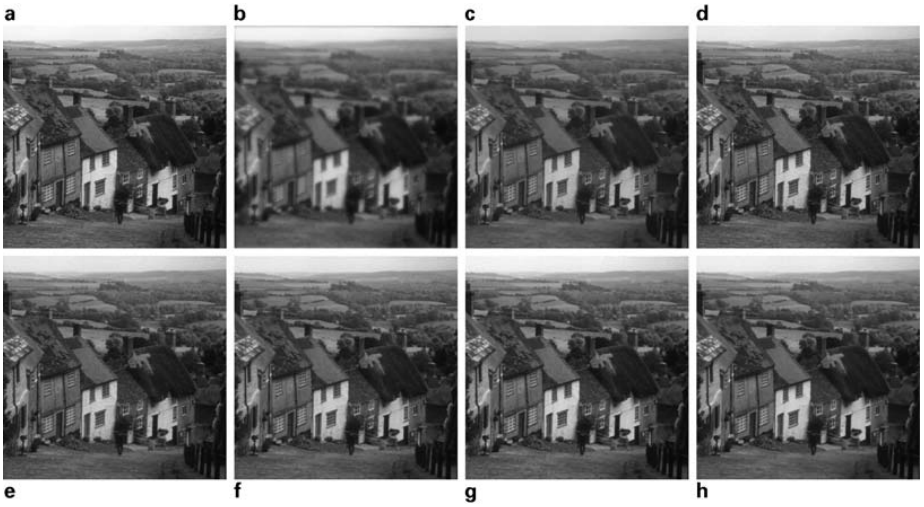

3 Image deblurring experiment with a 512×512 Gold Hill image: (a) original image; (b) blurred image; (c) ForWaRD result, ISNR = 4.51; (d) FTVd result, ISNR = 4.98; (e) ShearDec result, ISNR = 4.66; (f) L0-AbS result, ISNR = 5.02; (g) CGMK result, ISNR = 4.95; (h) our method result, ISNR = 5.22

The Imaging Science Journal ims356.3d 20/8/12 17:04:45
The Charlesworth Group, Wakefield +44(0)1924 369598 - Rev 7.51n/W (Jan 20 2003)

4 Details of the image deblurring experiment with a 512×512 Lena image: (a) original image; (b) blurred image; (c) ForWaRD result, ISNR = 3.74; (d) FTVd result, ISNR = 3.63; (e) ShearDec result, ISNR = 3.90; (f) L0-AbS result, ISNR = 4.11; (g) CGMK result, ISNR = 3.93; (h) our method result, ISNR = 4.27

variance of $\eta^2 = 6.76$, the region of support is 35×35, and the noise variance $\sigma^2 = 4$. The PSF was corrupted with additive white Gaussian noise of variance 8×10^{-7}, and the noise variance is estimated as $\sigma^2 = 6.5$. Four hundred independent realisations of the stochastic blurs were formed the common input to each method. From this experiment, one can see that our algorithm has good visual and objective quality. The ISNR values are summarised in Table. 2 under the Exp 6.

5 CONCLUSION AND FUTURE WORK

In this work, we have proposed an effective image deblurring method. The curvelet-based empirical Wiener shrinkage filter and the NLM filter are the exciting innovation and work well for images containing directionally oriented features. So our algorithm restores the blurred image by incorporating a curvelet-based empirical Wiener filter with a spatial-based joint NLM filter. We have compared

5 Image deblurring experiment with a 512×512 Lena image: (a) blurred image; (b) ForWaRD, ISNR = 2.34; (c) FTVd result, ISNR = 2.61; (d) ShearDec result, ISNR = 2.73; (e) L0-AbS result, ISNR = 2.87; (f) our final result, ISNR = 3.08

The Imaging Science Journal ims356.3d 20/8/12 17:04:57
The Charlesworth Group, Wakefield +44(0)1924 369598 - Rev 7.51n/W (Jan 20 2003)

the performance of the proposed method against the some state-of-the-art methods. Results have shown that the proposed method is attractive to obtain a deblurring result with better visual and quantitative performance.

It is also worth noting that many of the improved/fast NLM filter methods like[33,34] proposed to eliminate dissimilar pixels in the search window before computing their weight or to substitute with a more robust similarity metric to achieve better results or much speed-up. These ideas can be easily adopted into our method and will be in our future work.

REFERENCES

1 Guo, K., Lim, W., Labate, D., Weiss, G. and Wilson, E. Wavelets with composite dilations and their MRA properties. *Appl. Comput. Harmon. Anal.*, 2006, **20**, 231–249.

2 Mallat, S. A Wavelet Tour of Signal Processing, 1998 (Academic, New York).

3 Starck, J. L., Candès, E. J. and Donoho, D. L. The curvelet transform for image denoising. *IEEE Trans. Image Process.*, 2002, **11**, 670–684.

4 Candès, E. and Donoho, D. In Curves and Surfaces (Ed. A. Cohen, C. Rabut and L. L. Schumaker), 1999, pp. 105–120 (Vanderbilt University Press, Nashville, TN).

5 Candes, E., Demanet, L., Donoho, D. and Ying, L. X. Fast discrete curvelet transforms. *Multiscale Model. Simul.*, 2006, **5**, 861–899.

6 Donoho, D. L. Sparse components of images and optimal atomic decomposition. *Constr. Approx.*, 2001, **17**, 353–382.

7 Hennenfent, G., Herrmann, F. and Neelamani, R. Seismic deconvolution revisited with curvelet frames, Proc. EAGE 67th Conf. and Exhib., Madrid, Spain, June 2005, EAGE.

8 Candès, E. J. and Donoho, D. L. Recovering edges in ill-posed inverse problems: optimality of curvelet frames. *Ann. Statist.*, 2002, **30**, 784–842.

9 Buades, A., Coll, B. and Morel, J. M. A non-local algorithm for image denoising, Proc. IEEE Int. Conf. on *Computer vision and pattern recognition: CVPR 2005*, San Diego, CA, USA, June 2005, IEEE Computer Society, pp. 60–65.

10 Buades, A., Coll, B. and Morel, J. M. Nonlocal image and movie denoising. *Int. J. Comput. Vis.*, 2008, **76**, 123–139.

11 Katsaggelos, A. K. (Ed.) Digital Image Restoration, 1991 (Springer-Verlag, New York).

12 Hansen, P. C. Rank-deficient and Discrete Ill-posed Problems: Numerical Aspects of Linear Inversion, 1998 (SIAM, Philadelphia, PA).

13 Donoho, D. L. Nonlinear solution of linear inverse problems by wavelet-vaguelette decomposition. *Appl. Comput. Harmon. Anal.*, 1995, **2**, 101–126.

14 Neelamani, R., Choi, H. and Baraniuk, R. G. ForWaRD: Fourier-wavelet regularized deconvolution for ill-conditioned systems. *IEEE Trans. Signal Process.*, 2004, **52**, 418–433.

15 Patel, V. M., Easley, G. R. and Healy, Jr, D. M. Shearlet-based deconvolution. *IEEE Trans. Image Process.*, 2009, **18**, 2673–2685.

16 Yang, H. and Zhang, Z. B. Image deblurring based on ForIcM: Fourier shrinkage and incomplete measurements. *J. Imaging Sci.*, 2012, to be published.

17 Portilla, J. Image restoration through L0 analysis-based sparse optimization in tight frames, Proc. 16th IEEE Int. Conf. on *Image processing: ICIP 2009*, Cairo, Egypt, November 2009, IEEE, pp. 3909–3912.

18 Chantas, G., Galatsanos, N., Molina, R. and Katsaggelos, A. Variational bayesian image restoration with a product of spatially weighted total variation image priors. *IEEE Trans. Image Process.*, 2010, **19**, 351–362.

19 Gan, X. C., Liew, A. W.-C. and Yan, H. A POCS-based constrained total least squares algorithm for image restoration. *J. Vis. Commun. Image Represent.*, 2006, **17**, 986–1003.

20 Landweber, L. An iterative formula for Fredholm integral equations of the first kind. *Am. J. Math.*, 1951, **73**, 615–624.

21 Richardson, W. H. Bayesian-based iterative method of image restoration. *J. Opt. Soc. Am.*, 1972, **62**, 55–59.

22 Lucy, L. B. An iterative technique for the rectification of observed distributions. *Astron. J.*, 1974, **79**, 745–754.

23 Do, M. N. and Vetterli, M. The contourlet transform: an efficient directional multiresolution image representation. *IEEE Trans. Image Process.*, 2005, **14**, 2091–2106.

24 Dong, W. S., Zhang, L., Shi, G. M. and Wu, X. L. Image deblurring and super-resolution by adaptive sparse domain selection and adaptive regularization. *IEEE Trans. Image Process.*, 2011, **20**, 1838–1857.

25 Wang, Y., Yang, J., Yin, W. and Zhang, Y. A new alternating minimization algorithm for total variation image reconstruction. *SIAM J. Imag. Sci.*, 2008, **1**, 248–272.

26 Beck, A. and Teboulle, M. A fast iterative shrinkage-thresholding algorithm for linear inverse problems. *SIAM J. Imaging Sci.*, 2009, **2**, 183–202.

27 Bioucas-Dias, J. and Figueiredo, M. A new TwIST: two-step iterative shrinkage/thresholding algorithms for image restoration. *IEEE Trans. Imaging Process.*, 2007, **16**, 2992–3004.

28 Michailovich, O. V. An iterative shrinkage approach to total-variation image restoration. *IEEE Trans. Image Process.*, 2011, **20**, 1281–1299.

The Imaging Science Journal ims356.3d 20/8/12 17:05:08
The Charlesworth Group, Wakefield +44(0)1924 369598 - Rev 7.51n/W (Jan 20 2003)

29 Hillery, A. D. and Chin, R. T. Iterative Wiener filters for image restoration. *IEEE Trans. Signal Process.*, 1991, **39**, 1892–1899.

30 Ghael, S., Sayeed, A. M. and Baraniuk, R. G. Improved wavelet denoising via empirical Wiener filtering. *Proc. SPIE*, 1997, **3169**, 389–399.

31 Zhao, M., Zhang, W. and Wang, Z. L. Satellite image deconvolution based on nonlocal means. *Appl. Opti.*, 2010, **49**, 6286–6294.

32 Petschnigg, G., Agrawala, M., Hoppe, H., Szeliski, R., Cohen, M. and Toyoma, K. Digital photography with flash and no-flash image pairs. *ACM Trans. Graph.*, 2004, **23**, 664–672.

33 Vignesh, R., Oh, B. T. and Kuo, C.-C. J. Fast non-local means (NLM) computation with probabilistic early termination. *IEEE Signal Process. Lett.*, 2010, **17**, 277–280.

34 Wong, A., Fieguth, P. and Clausi, D. A perceptually adaptive approach to image denoising using anisotropic non-local means, Proc. 15th IEEE Int. Conf. on *Image processing: ICIP 2008*, San Diego, CA, USA, October 2008, IEEE, pp. 537–540.

The Imaging Science Journal ims356.3d 20/8/12 17:05:08
The Charlesworth Group, Wakefield +44(0)1924 369598 - Rev 7.51n/W (Jan 20 2003)

Authors Queries

Journal: **The Imaging Science Journal**
Paper: **356**
Title: **Image deblurring using empirical Wiener filter in the curvelet domain and joint non-local means filter in the spatial domain**

Dear Author
During the preparation of your manuscript for publication, the questions listed below have arisen. Please attend to these matters and return this form with your proof. Many thanks for your assistance

Query Reference	Query	Remarks
1	Please confirm the running head is correct.	
2	Please supply page/paper no. for Ref. 7.	
3	Please update the information for Ref. 16.	